
Chameleon: Adapting to Peer Images for Planting Durable Backdoors in Federated Learning

Yanbo Dai¹ Songze Li^{1,2}

Abstract

In a federated learning (FL) system, distributed clients upload their local models to a central server to aggregate into a global model. Malicious clients may plant backdoors into the global model through uploading poisoned local models, causing images with specific patterns to be misclassified into some target labels. Backdoors planted by current attacks are not durable, and vanish quickly once the attackers stop model poisoning. In this paper, we investigate the connection between the durability of FL backdoors and the relationships between benign images and poisoned images (i.e., the images whose labels are flipped to the target label during local training). Specifically, benign images with the original and the target labels of the poisoned images are found to have key effects on backdoor durability. Consequently, we propose a novel attack, Chameleon, which utilizes contrastive learning to further amplify such effects towards a more durable backdoor. Extensive experiments demonstrate that Chameleon significantly extends the backdoor lifespan over baselines by $1.2\times \sim 4\times$, for a wide range of image datasets, backdoor types, and model architectures.

1. Introduction

Rocketing development in computational resources brings exponential growth in both personal and corporate data. To sufficiently exploit these data and break the data isolation between decentralized data owners, collaborative training frameworks that respect data privacy and resist malicious participants are needed (Lyu et al., 2022). Federated learn-

ing (FL) (McMahan et al., 2017), consisting of a group of data-owning clients collaborating through a central server, is an emerging collaborative training paradigm, in which clients do not share their raw data with either the server or other clients, but participate in training a global model through uploading local models or gradients to the server. While protecting clients' data privacy, FL systems are vulnerable to a number of malicious attacks (Bagdasaryan et al., 2020; Zhang et al., 2022; Fang et al., 2020; Geiping et al., 2020; Fung et al., 2020; Shejwalkar et al., 2022; Nasr et al., 2019; Bhagoji et al., 2019), which hampers FL from being used in real-world settings.

Malicious clients can launch model poisoning attacks to damage the performance of the global model, via uploading deliberately manipulated local models. According to attacker's goals, model poisoning attacks can be categorized into untargeted attacks (Fang et al., 2020; Shejwalkar & Houmansadr, 2021; Chen et al., 2017b; Guerraoui et al., 2018) and backdoor attacks (Bhagoji et al., 2019; Bagdasaryan et al., 2020). Compared with untargeted attacks whose goal is to compromise the overall performance of the global model, backdoor attacks are especially destructive because of its strong stealth. Specifically, backdoor attackers try to have the global model misclassify to a particular target label when it encounters certain image patterns (or triggers), and perform normally on other inference tasks without triggers.

Previous works (Bagdasaryan et al., 2020; Zhang et al., 2022; Wang et al., 2020; Sun et al., 2019; Wen et al., 2022) have successfully planted backdoors in FL models. However, these works usually need attackers to keep uploading poisoned models to avoid planted backdoors from vanishing. This requires attackers to consistently participate in the training process, which will make the embedded backdoor easier to be detected. It has been observed in current attacks (Bagdasaryan et al., 2020; Zhang et al., 2022) that once all attackers leave the training procedure or the global model is retrained after malicious attacks stop, backdoors will quickly be erased by model updates from benign clients (Xie et al., 2021). In such cases, attackers wish to plant more durable backdoors to ensure that the inserted backdoors survive until the FL system is deployed.

¹IoT Thrust, Information Hub, Hong Kong University of Science and Technology (Guangzhou), Guangzhou, China
²Department of Computer Science and Engineering, Hong Kong University of Science and Technology, Hong Kong SAR, China.
Correspondence to: Songze Li <songzeli@ust.hk>.

As for the reason for rapidly vanishing backdoors, it is still not fully understood. Most previous works (Zhang et al., 2022; Wen et al., 2022) try to explain from the perspective of model conflicts. They argue that the poisoned model trained by the malicious client conflicts with benign models on certain key parameters. When attackers no longer send the poisoned model to the central server, following uploaded benign models will gradually erase the malicious client’s contribution on these parameters, and thus backdoor will vanish. (Wang et al., 2020) proposes edge-case attacks from the perspective of backdoor samples’ distribution. Also, they train the poisoned model using projected gradient descent, which periodically projects the model parameters on a ball centered around the model of the previous iteration, to escape the norm-clipping defense that mitigates the effect from abnormally large updates. They argue that backdoors trained by data samples that live in the tail of the input distribution are more durable and thus resistant to erasing. Because these edge samples have less chance to conflict with other samples.

In this work, we conduct first-principle investigations on the key factors that affect backdoor durability in FL, through the lens of relationships between sample images, and propose a new backdoor attack, Chameleon, which allows attackers to plant more durable visual backdoors *through adapting to peer images*. We observe that the durability of backdoors is mainly dominated by the presence of two types of peer benign images that are closely related to the poisoned images: 1) *interferers*: images that share the same original labels with the poisoned images; and 2) *facilitators*: images with target backdoor label. Interferers are much likely to cause update conflicts between the poisoned updates and benign updates, which may cause the drop of backdoor accuracy. Facilitators, on the other hand, can help to reintroduce the backdoor information to the FL model, and slow down the catastrophic forgetting effect after adversaries leave the training process. Motivated by this observation, we design Chameleon to amplify these effects on the backdoor durability.

Specifically, the local training process at a corrupted client is divided into two stages. In the first stage, contrastive learning is employed to train a representation encoder, such that the embedding distance between poisoned images and the interferers is pushed further, and the embedding distance between poisoned images and the facilitators is pulled closer. Without changing the network architecture, the second stage of Chameleon simply trains a classifier while fixing the parameters of the encoder obtained in the first stage.

We provide extensive empirical evaluations on multiple computer vision datasets, including CIFAR10, CIFAR100, and EMNIST, with both pixel-pattern backdoors and semantic backdoors (Bagdasaryan et al., 2020) against a FL system

equipped with norm-clipping defense (Sun et al., 2019). We show that Chameleon outperforms all the prior backdoor attacks in durability for both fixed and dynamic pattern backdoors, by increasing the backdoor lifespan by $1.2\times \sim 4\times$. Further, we also evaluate the performance of different backdoor attacks under different model architectures. We find that Chameleon is less sensitive to the change of model architecture and achieves strong backdoor durability consistently. In sharp contrast, backdoors inserted by prior methods fail to persist and fades quickly for deeper networks.

2. Related Work

Federated Averaging. FedAVG (McMahan et al., 2017) is the baseline algorithm for implementing FL systems. Generally speaking, FedAVG aims to minimize the summation of the local empirical losses $\sum_{i=1}^n F_i(\theta)$ of n participating clients, over a global model θ in a decentralized manner. For every global round t , the server broadcasts the current global model θ^t to a subset of randomly selected clients. Each selected client then optimizes its local loss $F_i(\theta)$ over local dataset, and uploads obtained local model θ_i^t back to the server. The central server then performs model aggregation to update the model $\theta^{t+1} = \frac{1}{n} \sum_{i=1}^n \theta_i^t$. In the rest of the paper, we will use FedAVG as our method to implement an FL system.

Backdoor Attacks. Backdoor attacks are initially proposed to poison deep learning models (Gu et al., 2019; Chen et al., 2017a; Liu et al., 2017; 2020; Shafahi et al., 2018; Saha et al., 2020). BadNets (Gu et al., 2019) first implements the backdoor attack by inserting pixel-pattern backdoors into deep learning models. In order to escape human examination on the malicious training dataset, (Chen et al., 2017a) further proposes an invisible attack method that generates backdoor images by blending the backdoor trigger with benign images. (Liu et al., 2017) explores optimized backdoor attacks which generate backdoor triggers through solving optimization problems. (Bagdasaryan et al., 2020) proposes the first backdoor attack targeting FL systems by uploading models with large norms to replace the original global model with the poisoned model. DBA (Xie et al., 2019) utilizes the decentralized nature of FL and achieves better performance by decomposing a global trigger pattern into separate local trigger patterns which are embedded into training dataset of multiple malicious parties.

Defenses. According to (Rieger et al., 2022a), defenses against backdoor attacks in FL can mainly be categorized into influence reduction approaches that constrain the impact of individual updates (Sun et al., 2019; Andreina et al., 2021; Naseri et al., 2022; Yin et al., 2018) and detection and filtering approaches that aim to identify and exclude poisoned updates (Nguyen et al., 2022; Rieger et al., 2022b; Shen et al., 2016; Zhao et al., 2020). Among all the defense

approaches, the norm-clipping defense proposed in (Sun et al., 2019) is the most widely adopted method. It regularizes the norm of each model update received at the server within a norm bound ρ , which was shown to be especially effective in mitigating model replacement backdoors (Bagdasaryan et al., 2020). There are also some general Byzantine-resistant mechanisms including Krum (Blanchard et al., 2017), Bulyan (Guerraoui et al., 2018), trimmed mean and median (Yin et al., 2018), which nevertheless focus more on defending untargeted attacks.

Visual Contrastive Learning. Contrastive learning, applied in computer vision tasks, is first proposed to handle unsupervised visual embedding learning problems. Moco (He et al., 2020) tries to encode images into key vectors and query vectors. By increasing the similarity between every query vector and its corresponding key vector and decreasing the similarity with other key vectors during training, visual representations with valuable information can be learned. SimCLR (Chen et al., 2020) adopts contrastive learning in self-supervised learning by using data augmentation. SupCon (Khosla et al., 2020) further utilizes contrastive learning in the supervised setting, which can effectively leverage label information, to improve the model prediction accuracy.

3. What affects backdoor durability in FL?

In this section, we investigate what affects the durability of backdoors in FL from the perspective of image samples. Instead of trying to explain the vanishing of the backdoors through analyzing interactions between poisoned and benign models, we focus on the impacts of the different relationships among images. In the following part, we define *peer images* as samples who have particular relationships with poisoned images. Further, we identify two types of *peer images* as *interferers* which share the same label with the original label of the poisoned images, and *facilitators* which share the same label with the target label. For example, consider an attacker whose goal is to make the FL model misclassify any green car image as a dog. In this scenario, all car images except for green car images are interferers and all dog images are facilitators. Next, we proceed to reveal the influence of peer images on the durability of backdoors, through carefully designed experiments.

We consider an FL system running an image classification task on CIFAR10 (Krizhevsky et al.), which is attacked by an extremely strong attacker who can perfectly replace the global model with a poisoned model through model replacement attack (Bagdasaryan et al., 2020). The poisoned model is trained following (Bagdasaryan et al., 2020), through creating a malicious training dataset by mixing poisoned images with benign images and perform local training as FedAVG. The attacker’s goal is to make the system misclas-

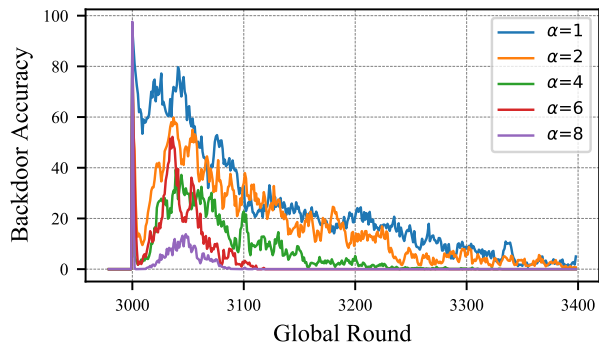


Figure 1. Backdoor accuracy with different percentages ($\alpha N/B$) of poisoned images in every training batch. The attacker performs model replacement attack at 3000th global round.

sify any car-with-vertically-striped-walls-in-the-background image as a bird. A total of $N(N = 7)$ poisoned images can be used for training. The attacker trains the poisoned model using mini-batch stochastic gradient descent with batch size $B(B = 64)$. The attacker mixes up αN poisoned images and other benign images in every training batch. The variation of backdoor accuracy with global round for different α is shown in Figure 1. The increase in the percentage of poisoned images both lowers the average accuracy and shortens the lifespan of the poison task. Training the poisoned model using only poisoned images make the model overfit, and the planted backdoor is easier to be erased by any other images. Without involving interferers in the backdoor training, the poisoned model does not pick up the difference between poisoned images and interferers as these two types of images have similar visual features. Thus, the following uploaded benign gradients from interferers are much more likely to conflict with the poisoned model, and then the inserted backdoor fades quickly.

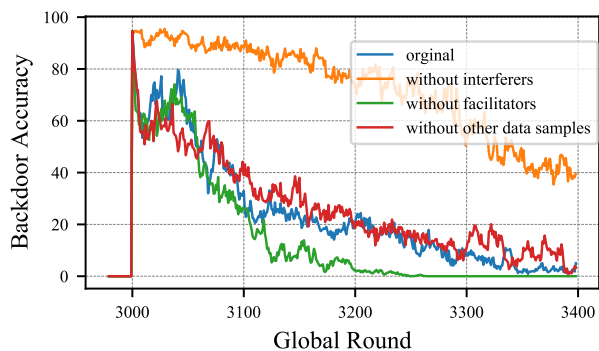


Figure 2. Backdoor accuracy with different dataset settings of the following uploaded benign models. The attacker performs model replacement attack at 3000th global round.

We consider another scenario that has the same basic setting as the previous one. Instead, we fix the training dataset of the malicious client by setting $\alpha = 1$ and change the

training datasets of the following selected benign clients. We deliberately remove certain types of data from the datasets of benign clients to test their effects on backdoor accuracy. As is shown in Figure 2, the persistence of the poison task can be significantly enhanced if there are no interferers in the dataset of the following benign clients. However, the lack of facilitators in the dataset of the following benign clients will lead to a decrease in the backdoor durability. Apart from these two types of data, the absence of any other data has minimum influence on the persistence of the backdoor task.

These experimental results illustrate how backdoor durability is affected by interactions between poisoned images with its peer images. Mixing poisoned images and the benign ones in backdoor training helps to enhance the lifespan of the inserted backdoor. Also, interferers and facilitators play crucial but completely different roles on influencing backdoor durability. We further elaborate in the following.

Update conflict with interferers. Let the encoder denotes the backbone network of the model. Also, let $T = t_1$ be the global round at which the attacker begins poisoning and $T = t_2$ be the global round in which the attacker finishes lpoisoning. For every poisoned image, it shares similar visual features with interferers (the green car and normal car for example). Without explicit regularization which can guide the encoder to discriminate poisoned data samples from interferers, the encoder may give analogous embedding for them. With analogous embedding and different assigned labels, the updated gradients of poisoned samples and interferers are in conflict. In such case, interferers will inevitably damage poison task performance when $T \in [t_1, t_2]$ and quickly erase the backdoor when $T > t_2$.

Slowdown of catastrophic forgetting by facilitators. Catastrophic forgetting refers to the defect of neural networks in learning tasks in a sequential fashion (Kirkpatrick et al., 2017). Neural networks are inclined to forget previous tasks once the data of these tasks is no longer provided. Similarly, catastrophic forgetting also damages the durability of poison tasks since poisoned images are no longer provided once the attacker leaves the FL system. In the long term, no matter how strong the attacker is, its embedded backdoor will inevitably be erased by the effect of catastrophic forgetting. However, this forgetting effect can be alleviated by facilitators possessed by benign clients. Facilitators, which have the same label as the backdoor target label, in the datasets of following participating benign clients will reintroduce the backdoor information to the global model and extend the lifespan of the inserted backdoor for $T > t_2$.

Motivated by the above observations, the durability of backdoors can be enhanced by leveraging sample relationships between poisoned images and peer images. Specifically, including interferers in the malicious training and making

Algorithm 1 Chameleon

Input: benign dataset: D_b , target label: y_t , backdoor type: t_{bk} , learning rate in training stage 1 and stage 2: η_1, η_2 , local batch size: B , number of local training rounds in stage 1 and stage 2: R_1, R_2 , local model parameters: $\theta = (\theta_{enc}, \theta_{cla})$, where θ_{enc} and θ_{cla} are the parameters of the encoder and the classifier respectively.

Data Preparation Stage:

poisoned data $x_p = \text{CreatePoisonedImg}(t_{bk})$
 poisoned label $y_p = y_t$
 poisoned dataset $D_p \leftarrow [(x_p, y_p)]$
 malicious training dataset $D \leftarrow \text{Mix}(D_b, D_p)$

Adaptation Stage:

for local training round $r = 1, \dots, R_1$ **do**
 $\mathcal{B}_1 \leftarrow (\text{split } D \text{ into batches of size } B)$
for $b_1 \in \mathcal{B}_1$ **do**
 $\theta_{enc} = \theta_{enc} - \eta_1 \nabla \mathcal{L}_{\text{SupCon}}(\theta_{enc}; b_1)$
end for
end for

Projection Stage:

$\theta_{enc} \leftarrow \text{FreezeParams}(\theta_{enc})$
for local training round $r = 1, \dots, R_2$ **do**
 $\mathcal{B}_2 \leftarrow (\text{split } D \text{ into batches of size } B)$
for $b_2 \in \mathcal{B}_2$ **do**
 $\theta_{cla} = \theta_{cla} - \eta_2 \nabla \mathcal{L}_{\text{CE}}(\theta_{cla}; \theta_{enc}, b_2)$
end for
end for
 return $\theta = (\theta_{enc}, \theta_{cla})$ to server

the poisoned images more distinct from the interferers helps the backdoor to last longer. Also, the forgetting effect on backdoors can be further slowed down by making poisoned images more similar to the facilitators. We next propose a novel backdoor attack, Chameleon, to achieve these goals by carefully designing the poisoned dataset, and utilizing contrastive learning in local training to adjust the distances between poisoned images and peer images in favor of a more durable backdoor.

4. Enhancing Backdoor Durability Utilizing Sample Relationships

4.1. Threat Model

Attacker’s Capability. We consider a FL system running image classification tasks, and assume that the attacker can attack the system in a continuous fashion for AttackNum global rounds. In each round, the attacker can corrupt one client. Once corrupted, the attacker has the full control over the training and model uploading process. We also assume

that the system is equipped with norm-clipping defense to eliminate anomalous model updates with irregularly large norms.

Attacker’s Goal. The attacker aims to plant different types of visual backdoors, including pixel-pattern backdoors and semantic backdoors (Bagdasaryan et al., 2020), into the FL model to make the model misclassify on a certain type of data while leaving other tasks uninfluenced. Further, the attacker would like the embedded backdoor persist as long as possible. Following (Zhang et al., 2022), we use Lifespan to measure the durability of the embedded backdoor.

Definition 3.1 (Lifespan). Let t_0 be the index of the global round on which the attacker finishes poisoning. Let γ be the backdoor threshold accuracy, θ_G^t be the global model parameters on global round t , $f(\cdot)$ be the accuracy function, and let D_{test} be the test set that contains poisoned images. We can define the γ -Lifespan $L(\gamma)$ of the backdoor as:

$$L(\gamma) = \max\{t | f(\theta_G^t, D_{\text{test}}) > \gamma\} - t_0 \quad (1)$$

4.2. Chameleon

We now introduce our new visual backdoor attack method, Chameleon, which improves backdoors’ durability by utilizing the relationships between poisoned images and peer images. In our method, the attacker first prepares a poisoned dataset that mixes benign images and poisoned images. Then, the training on the malicious client proceeds in an adaptation stage and a projection stage. In the adaptation stage, we utilize the contrastive learning paradigm to adjust embeddings of poisoned images and peer images to improve backdoor durability. The projection stage further trains a classifier for specific tasks after freezing the parameters of the encoder learnt from the previous stage. Notably, there is no architecture change between the poisoned model and the global model. Algorithm 1 describes Chameleon in details.

We define $E(\cdot)$ to be the representation encoder which maps input sample \mathbf{x} to a embedding vector $\mathbf{z} \in \mathbb{R}^d$, and $F(\cdot) = (E(\cdot), C(\cdot))$ to be the deep learning network trained at the clients that starts with $E(\cdot)$ and ends with a classifier $C(\cdot)$.

Data Preparation Stage. Let D_b , D_p be the benign and poisoned datasets, and (\mathbf{x}_b, y_b) , (\mathbf{x}_p, y_p) be the benign and poisoned data-label pairs respectively. Poisoned data \mathbf{x}_p is constructed according to different types of backdoors (pixel-pattern and semantic), and poisoned label y_p is the target label. The malicious training dataset \mathcal{D} of size N is then constructed by mixing up samples from both the benign dataset D_b and the poisoned dataset D_p . Exact mix rates are decided according to specific tasks.

Adaptation Stage. In the first training stage, the corrupted client trains the representation encoder $E(\cdot)$ using supervised contrastive learning (Khosla et al., 2020). The corre-

sponding loss function is defined as:

$$\mathcal{L}_{\text{SupCon}} = \sum_{i \in I} -\frac{1}{|S(i)|} \sum_{s \in S(i)} \log \frac{\beta(i) \exp(\mathbf{z}_i \cdot \mathbf{z}_s / \tau)}{\sum_{a \in I \setminus \{i\}} \exp(\mathbf{z}_i \cdot \mathbf{z}_a / \tau)}, \quad (2)$$

where $I = \{1, \dots, N\}$ is the index set of the malicious training dataset \mathcal{D} , and $S(i)$ is the set of the indices of all samples which share the same label with sample i . Also, \mathbf{z}_i is the normalized embedding computed by $E(\mathbf{x}_i)$ for the input sample \mathbf{x}_i , and $\beta(i)$ is the weight specifically designed for guiding the encoder to focus more on learning similar embeddings for poisoned images and facilitators. Explicit value of $\beta(i)$ for sample i is defined as:

$$\beta(i) = \begin{cases} \beta & y_i = y_p \\ 1 & y_i \neq y_p \end{cases}, \quad (3)$$

where y_i is the label of sample i , y_p is the poisoned label, and $\beta > 1$ is some design parameter.

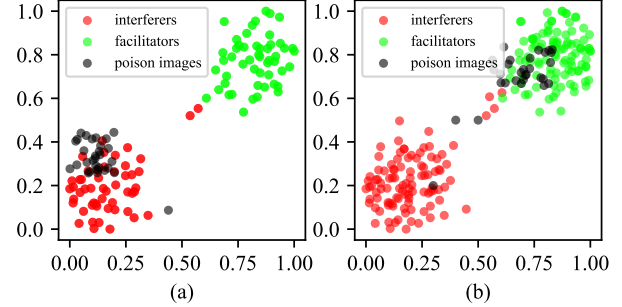


Figure 3. Illustration of the 2D embeddings, which are generated using t-SNE (Van der Maaten & Hinton, 2008), of poisoned images, interferers and facilitators obtained by (a) running the local training of FedAVG and (b) Chameleon.

Let I_p , I_{Fac} , I_{Int} be the index set of poisoned samples, facilitator samples and interferer samples respectively. For poisoned sample $i \in I_p$, facilitator sample $j \in I_{\text{Fac}}$ and interferer sample $k \in I_{\text{Int}}$, the dot product $\mathbf{z}_i \cdot \mathbf{z}_j$, $\mathbf{z}_i \cdot \mathbf{z}_k$ of the normalized embeddings of sample i , j , k can be seen as the correlation measure of the embeddings between poisoned images and peer images. Optimizing the encoder using the supervised contrastive loss function can drive $\mathbf{z}_i \cdot \mathbf{z}_j$ to become larger and $\mathbf{z}_i \cdot \mathbf{z}_k$ to become smaller. Thus, the distance of learned embeddings between poisoned samples and interferers are pushed farther and that between poisoned samples and facilitators are pulled closer. As illustrated in an example in Figure 3, compared with normal FedAVG that generates similar embeddings for poisoned images and their interferers (Figure 3(a)), the adaptation stage of Chameleon moves the poisoned images away from interferers and closer

to facilitators (Figure 3(b)). This helps to both alleviate the update conflict with interferers and strengthen the reintroduction effect of facilitators to compensate for catastrophic forgetting, thus expanding the lifespan of backdoors.

Projection Stage. In the second training stage, the attacker freezes the parameters of the encoder $E(\cdot)$ obtained from the previous stage, and trains a classifier $C(\cdot)$ using the cross-entropy loss \mathcal{L}_{CE} over D for classification tasks.

5. Experiments

In this section, we provide an extensive empirical evaluation of three different computer vision datasets, CIFAR10, CIFAR100 (Krizhevsky et al., 2009) and EMNIST (Cohen et al., 2017), by planting both pixel-pattern and semantic image backdoors (Bagdasaryan et al., 2020) with different FL settings.

We compare with state-of-the-art FL backdoor attacks, including baseline (Bagdasaryan et al., 2020), Neurotoxin (Zhang et al., 2022), and Anticipate (Wen et al., 2022):

- **Baseline** simply creates the malicious dataset by mixing poisoned images with benign images, and performs local training using projected gradient descent (Wang et al., 2020).
- **Neurotoxin** tries to improve the durability of the inserted backdoors by identifying the parameters which are not frequently updated by benign clients and inserting backdoors using these parameters.
- **Anticipate** tries to improve the durability of backdoors by considering future model updates from benign clients in the training process of the corrupted client.

5.1. Experiment Setup

Our experiment implements all the tasks in a FL system running image classification task using FedAVG (McMahan et al., 2017), on a single machine using an NVIDIA GeForce RTX 3090 GPU with 24GB memory. The implemented FL system is assumed to be equipped with norm-clipping defense and the clipping bound ρ is chosen as the maximal value that does not damage the model’s convergence performance.

Ten randomly selected clients contribute at every aggregation round while the total number of clients is 100. For all three datasets, we randomly split the dataset over clients in a non-iid manner (typical in FL), using Dirichlet sampling with the parameter α set to 0.9 by default (Hsu et al., 2019). The durability of backdoor attack methods on certain datasets is evaluated using the γ -Lifespan $L(\gamma)$ under certain poison accuracy threshold γ .

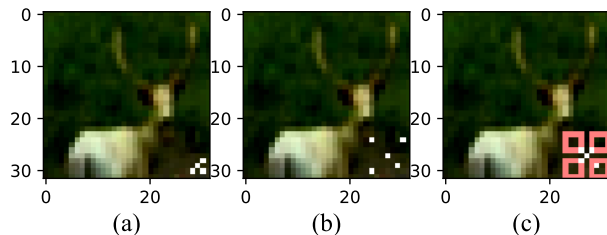


Figure 4. (a) Type-1 pixel-pattern backdoor. (b) Type-2 pixel-pattern backdoor. (c) Illustration of possible pixel locations of type-2 pixel-pattern backdoor.

Pixel-pattern backdoors. In this work, we investigate two different types of pixel-pattern backdoors. We choose the first type from (Gu et al., 2019), where as shown in Figure 4(a), a fixed pixel-pattern is overlaid with the original image. We also consider a second type to be a dynamic one with the central pixel fixed and locations of the four pixels in the corners are randomly generated within a certain range. One such example is given in Figure 4(b). In general, as illustrated in Figure 4(c), four pixels in the corners can only be generated within its own red box. The coordinates of the corner pixel (x_e, y_e) is generated as follow:

$$(x_e, y_e) = (x_c \pm (r_c \cdot \text{Random}(0, p_d) + 1), y_c \pm (r_c \cdot \text{Random}(0, p_d) + 1)), \quad (4)$$

where (x_c, y_c) is the coordinate of the central pixel, $\text{Random}(a, b)$ returns a random number between a and b , r_c is the maximal range of the corner pixel’s coordinate, and p_d represents the pattern diffusion level. With higher p_d , the inserted pixel patterns across different poisoned images are more diffused. The sign in Equation 4 is decided according to the specific location of the corner pixel.

For type-1 pixel-pattern backdoors, we randomly choose images from CIFAR10 and EMNIST and overlay type-1 pixel-pattern triggers on the images to form the poisoned dataset. For type-2 pixel-pattern backdoors, images from CIFAR10 are randomly chosen to be poisoned images with two different pattern diffusion levels $p_d = 0.1, 0.5$. Poisoned images of CIFAR10 are expected to be classified as birds (label 2) and poisoned images of EMNIST are expected to be classified as number 2 (label 2). We use ResNet18 for these tasks.

Semantic backdoors can be chosen as any naturally occurring feature of the physical scene and do not require attackers to modify the original images. Following (Bagdasaryan et al., 2020), we choose green-car, car-with-racing-stripes and car-with-vertically-striped-walls-in-the-background as our semantic backdoors for CIFAR10. All poisoned images in CIFAR10 are expected to be predicted as birds (label 2). Additionally, we choose truck-with-vertically-striped-walls-in-the-background and bicycle-with-black-background as

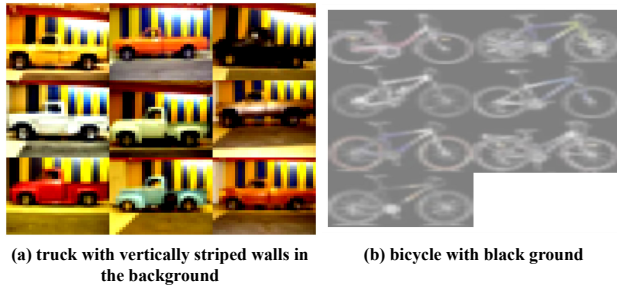


Figure 5. Examples of semantic backdoors for CIFAR100 (a) truck-with-vertically-striped-walls-in-the-background. (b) bicycle-with-black-background.

our semantic backdoors for CIFAR100 as shown in Figure 5. Poisoned images with each of the two semantic backdoors are expected to be predicted as butterfly (label 14) and castle (label 17) respectively. We use ResNet18 for these tasks.

Model architecture. We also evaluate the performance of backdoor attacks under different model architectures, including ResNet18 and ResNet34. We use car-with-vertically-striped-walls-in-the-background and car-with-racing-stripes in CIFAR10 as our semantic backdoors.

5.2. Results

We present representative results in this section, and leave the others to Appendix A due to space constraint. We find that in all experiments, Chameleon plants more durable backdoors than all other attacks.

Chameleon improves durability significantly under different settings. Figure 6 presents the results of the performance of different pixel-pattern backdoors on CIFAR10. Chameleon achieves the longest 50%-Lifespan under all considered pixel-pattern settings in Figure 6(a)-(c). We can also see from Figure 6(d) that type-1 backdoor persists longer than type-2, and the durability of type-2 reduces as p_d increases. This indicates that backdoors with more diffused and dynamic features are more difficult to plant and are more inclined to vanish. This is because that it becomes harder for the poisoned model to capture backdoor features and learn similar embeddings of poisoned images and facilitators. Thus, the reintroduction effect of facilitators becomes weaker and the lifespan declines.

For semantic backdoor experiments, Chameleon improves backdoor durability by $2.8 \times \sim 4 \times$ over prior methods. For two semantic backdoors on CIFAR10, as shown in Figure 7(a) and (b), the 50%-Lifespans for Chameleon are 1106 and 264, and the max 50%-Lifespans of the rest three attack methods are 283 and 70, respectively. We also note that the durability of the car-with-racing-stripes backdoor is weaker than the car-with-vertically-striped-walls-in-the-background backdoor in Figure 7. Similar to the pixel-pattern backdoor,

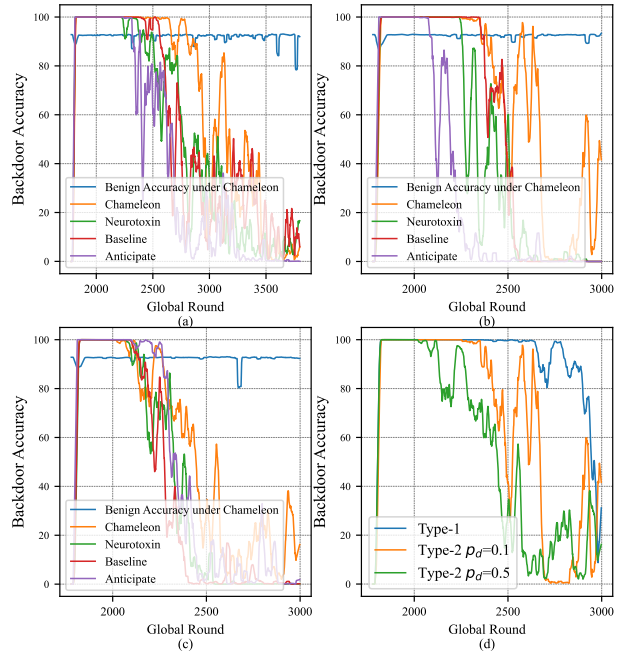


Figure 6. Backdoor accuracy on CIFAR10 with (a) Type 1 pixel-pattern backdoor, (b) Type 2 pixel-pattern backdoor with $p_d = 0.1$, (c) Type 2 pixel-pattern backdoor with $p_d = 0.5$. (d) Chameleon planting pixel-pattern backdoors with different feature diffusion levels. For all tasks, the attack starts at round 1800, and lasts for AttackNum=40 rounds.

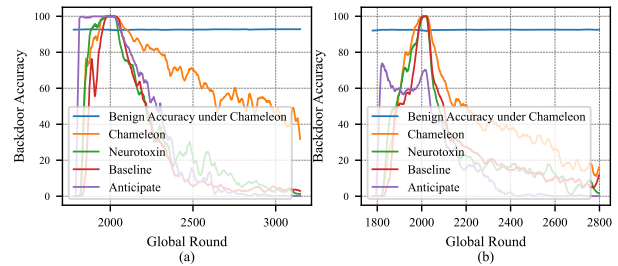


Figure 7. Backdoor accuracy on CIFAR10 with (a) car-with-vertically-striped-walls-in-the-background, (b) car-with-racing-stripes. For all tasks, the attack starts at round 1800, and lasts for AttackNum=230 rounds.

this is because the backdoor features of car-with-racing-stripes images are more diffused (the location and color of the racing stripe are more diverse across poisoned images) than the backdoor features of car-with-vertically-striped-walls-in-the-background images (the location and color of the vertically striped walls are more uniform across poisoned images). We note that in Figure 7(b), Anticipate even fails to achieve 100% backdoor accuracy right after backdoor injection. For CIFAR100 task in Figure 8, the 50%-Lifespan for Chameleon is 661, improving the max 50%-Lifespan of the rest three attacks (229) by $2.88 \times$.

Chameleon improves durability under existing defense

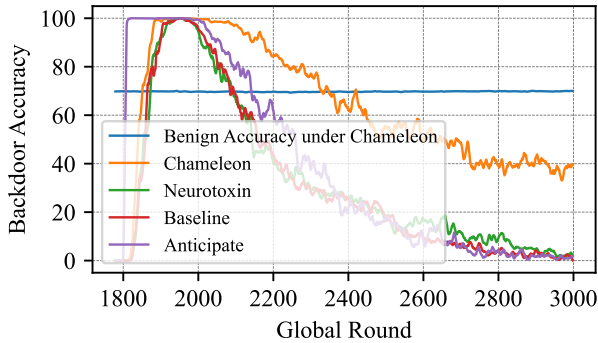


Figure 8. Backdoor accuracy on CIFAR100 with bicycle-with-black-background. For this task, the attack starts at round 1800, and lasts for AttackNum=150 rounds.

Table 1. 50%-lifespan of the backdoor inserted by different methods (A) Chameleon, (B) Anticipate, (C) Neurotoxin, and (D) Baseline, under different defense methods. Here, - for Anticipate means the method fails to insert backdoor to the FL system under the evaluated defenses. The evaluated backdoor is bicycle-with-black-background samples in CIFAR100.

Defenses	(A)	(B)	(C)	(D)
NCD only	661	229	112	133
Weakly DP & NCD	150	68	47	-
Krum & NCD	72	-	53	57
FLAME & NCD	102	-	30	17

methods. Table 1 demonstrates the effectiveness of our method against three different defense methods: weakly DP (Sun et al., 2019) which is widely adopted in FL defense; Krum (Blanchard et al., 2017) which is the most well-known Byzantine-robust aggregation rule; and FLAME (Nguyen et al., 2022) which is the SOTA backdoor defense method. Under the evaluated defense methods, the durability of the backdoor inserted using Chameleon decreases, compared to the setting where there is only norm-clipping defense (NCD). However, Chameleon still achieves the longest backdoor lifespan among all evaluated methods for the same defense.

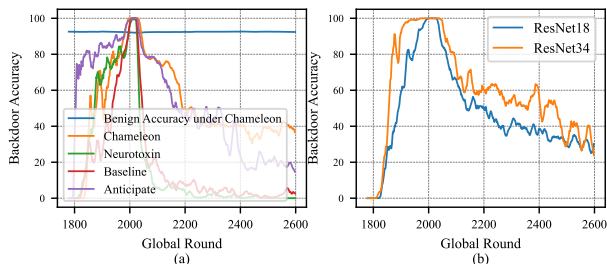


Figure 9. (a) Backdoor accuracy using Chameleon on CIFAR10 with car-with-vertically-striped-walls-in-the-background. The model architecture used here is ResNet34. (b) Backdoor accuracy on CIFAR10 with car-with-racing-stripes. The backdoor durability with different model architectures are evaluated. For all tasks, the attack starts at round 1800, and lasts for AttackNum=230 rounds.

Chameleon is less sensitive to model architectures. Comparing Figure 7(a) and Figure 9(a), we can see that the model architecture could directly influence the durability of the inserted backdoor. The 40%-Lifespans for baseline, Neurotoxin reduces from 215, 221 to 13, 7 respectively after the model architecture changes to ResNet34. While the 40%-Lifespan for Chameleon reduces from 1120 to 567 which is still the longest among all the evaluated attack methods. This demonstrates that compared to prior methods, Chameleon is less sensitive to model architecture and is more suitable for attacking more sophisticated models. Interestingly, for backdoors with more diffused features, the durability of backdoors planted by Chameleon improves when the model architecture changes from ResNet18 to ResNet34 in Figure 9(b). We envision that this is because that deeper models possess stronger learning ability to assign distinct embeddings for poisoned images and interferers, and assign similar embeddings for poisoned images and facilitators when the backdoor features get more diffused.

Table 2. Benign accuracy of the main task on CIFAR10 when Chameleon semantic backdoors (A) car-with-vertically-striped-walls-in-the-background, (B) green-car, and (C) car-with-racing-stripes are planted into the FL system.

Benign accuracy when	(A)	(B)	(C)
Start Attack	92.55%	92.48%	92.05%
Stop Attack	92.25%	92.59%	92.00%

Chameleon is stealthy and does not degrade benign accuracy. Table 2 provides the benign accuracy of the main task when the Chameleon attacker plants semantic backdoors into CIFAR10 task. We can see that injecting backdoors do not affect the benign accuracy, which shows that Chameleon is stealthy against human examination on benign accuracy.

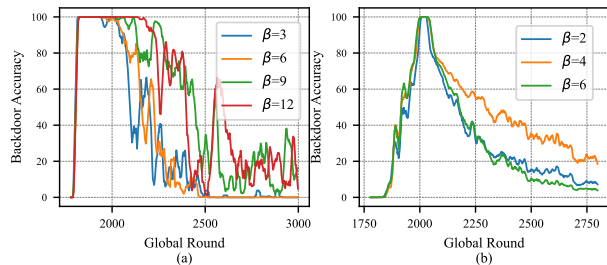


Figure 10. The influence of hyper-parameter β with different values on the persistence of the inserted (a) type-2 pixel-pattern backdoor with $p_d = 0.5$ and (b) semantic backdoor with car-with-racing-stripes trigger. For all tasks, the attack starts at round 1800, and lasts for AttackNum=40, 230 rounds respectively.

Chameleon is effective under different data non-iid settings. When clients’ data distribution becomes more non-iid, adversaries may possess fewer interferer and facilitator

Table 3. 50%-lifespan of backdoor inserted by different methods under the assumption that data held by different clients in FedAVG is partitioned using Dirichlet sampling with parameter α .

α	Chameleon	Anticipate	Neurotoxin
0.9	661	229	112
0.5	261	193	230
0.2	393	137	214

Table 4. 50%-lifespan of backdoor inserted by different methods under the assumption that data held by different clients in FedProx is partitioned using Dirichlet sampling with parameter α .

α	Chameleon	Neurotoxin
0.9	1522	472
0.5	422	187
0.2	508	250

samples, which may shorten the lifespan of the embedded backdoor. In this case, we can assume that adversaries can manage to collect a small auxiliary dataset \mathcal{D}_{aux} which contains interferer and facilitator samples. Malicious clients can then incorporate a certain number of interferer and facilitator samples drawn from the auxiliary dataset into every training batch to ensure that the embedding of the learnt backdoor is away from that of interferers and close to that of facilitators.

The lifespans of multiple backdoor attacks under different degrees of data non-iidness are presented in Table 3 for FedAVG and in Table 4 for FedProx (Li et al., 2020), which is a popular FL protocol to mitigate model bias due to non-iid data distribution. We can find that for both FedAVG and FedProx, the durability of the evaluated backdoor, bicycle-with-black-background samples in CIFAR100, inserted by Chameleon is the strongest among all evaluated attacks, for all different values of α . Also, for the same value of α , Chameleon introduces more durable backdoor in FedProx, compared with FedAVG.

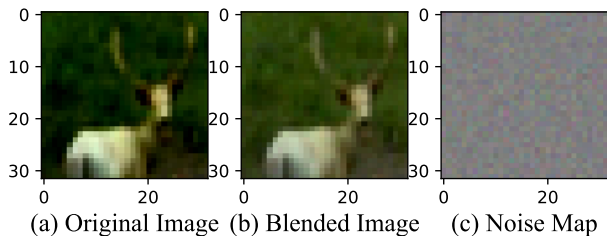


Figure 11. (a) Original image. (b) Blended image which is the composition of the original image and the noise map. (c) Noise map which is also the backdoor trigger. The noise map is fixed during the entire process.

Chameleon is effective to insert more advanced backdoors. We further provide experimental results on the durability of the blended backdoor (Chen et al., 2017a) and the targeted contamination attack (TCA) (Tang et al., 2021)

Table 5. 50%-lifespan of the evaluated backdoors inserted by different methods.

Backdoor	Chameleon	Neurotoxin	Baseline
Blended	184	60	40
TCA	1566	949	627

using different methods. The backdoor trigger chosen for blended backdoor is the randomly generated noise map with mean 0 and variance 0.05. In this scenario, as shown in an example in Figure 11, the backdoor images look almost identical to the benign ones. The backdoor trigger pattern for the targeted contamination backdoor is the same pixel-pattern trigger as that from BadNets (Gu et al., 2019). However, instead of being source-agnostic, which means that the poisoned model assigns the target label to samples with backdoor trigger regardless of their original labels, the TCA is source-specific, which only assigns the target class to trigger-carrying samples from certain classes. From Table 5 we can see that the durability of the backdoor inserted by Chameleon is still the strongest among the evaluated methods, for these two advanced backdoors.

Ablation study on β . We investigate the influence of choosing different β , which is the hyper-parameter in the contrastive learning loss function in (2), on the durability of Chameleon backdoors. Figure 10 shows the influence of different β on pixel-pattern backdoor and semantic backdoor.

As shown in Figure 10(a), the durability of type-2 pixel-pattern backdoor improves monotonically as β increase from 3 to 12. Whereas for semantic backdoor in Figure 10(b), the strongest durability is achieved with an intermediate value of $\beta = 4$. This can be explained from the internal difference between pixel-pattern backdoors and semantic backdoors. For pixel-pattern backdoors, the attacker need to overlay carefully chosen triggers on the original images to generated poisoned images. It is thus easier for the poisoned model to learn the difference between poisoned images and interferers, and assigns more distinct embeddings for them. Update conflicts with interferers are then significantly alleviated. In this case, the attacker can improve backdoor durability mainly through strengthening the reintroduction effect of facilitators, and this can be achieved by increasing β to further pull closer embeddings of poisoned images and facilitators during contrastive learning. However, update conflicts with interferers are more severe in semantic backdoors as we do not insert new backdoor trigger and consider some naturally occurring feature as the backdoor trigger. This makes assigning distinct embeddings for poisoned images and interferers more difficult, and update conflicts with interferers can greatly damage the durability in this case. Unlike the case of the case of pixel-pattern backdoors, increasing β introduces contradictory effects on moving away from interferers and moving

towards facilitators. Therefore, to maximize backdoor durability, a value of β that strikes a good balance between these two effects should be chosen.

6. Discussion and Conclusion

Notably, the main focus of Chameleon is to extend the lifespan of backdoors in FL but not in general to escape all advanced backdoor defenses. We envision that future researches that aim to escape from advanced defenses can combine with our method to improve the durability of the inserted backdoors.

In this paper, we find that utilizing the sample relationships can greatly enhance the durability of the inserted visual backdoor in FL. Based on the observation, we developed a novel attack method, Chameleon, which adopts contrastive learning paradigms to adjust the relative embedding relationship among poisoned samples, interferers, and facilitators to improve the durability of backdoors. Over evaluations for a wide range of datasets, backdoor types and model architectures, we show that Chameleon are consistently durable and can improve the backdoor durability by $1.2\times \sim 4\times$ compared to prior methods.

Acknowledgement

This work is in part supported by the National Nature Science Foundation of China (NSFC) Grant 62106057, Foshan HKUST Projects FSUST20-FYTRI04B, and Guangzhou Science and Technology City-University Joint Project 2023A03J0151.

References

- Andreina, S., Marson, G. A., Möllering, H., and Karame, G. Baffle: Backdoor detection via feedback-based federated learning. In *2021 IEEE 41st International Conference on Distributed Computing Systems (ICDCS)*, pp. 852–863. IEEE, 2021.
- Bagdasaryan, E., Veit, A., Hua, Y., Estrin, D., and Shmatikov, V. How to backdoor federated learning. In Chiappa, S. and Calandra, R. (eds.), *Proceedings of the Twenty Third International Conference on Artificial Intelligence and Statistics*, volume 108 of *Proceedings of Machine Learning Research*, pp. 2938–2948. PMLR, 26–28 Aug 2020.
- Bhagoji, A. N., Chakraborty, S., Mittal, P., and Calo, S. Analyzing federated learning through an adversarial lens. In *International Conference on Machine Learning*, pp. 634–643. PMLR, 2019.
- Blanchard, P., El Mhamdi, E. M., Guerraoui, R., and Stainer, J. Machine learning with adversaries: Byzantine tolerant gradient descent. *Advances in Neural Information Processing Systems*, 30, 2017.
- Chen, T., Kornblith, S., Norouzi, M., and Hinton, G. A simple framework for contrastive learning of visual representations. In *International conference on machine learning*, pp. 1597–1607. PMLR, 2020.
- Chen, X., Liu, C., Li, B., Lu, K., and Song, D. Targeted backdoor attacks on deep learning systems using data poisoning. *arXiv preprint arXiv:1712.05526*, 2017a.
- Chen, Y., Su, L., and Xu, J. Distributed statistical machine learning in adversarial settings: Byzantine gradient descent. *Proceedings of the ACM on Measurement and Analysis of Computing Systems*, 1(2):1–25, 2017b.
- Cohen, G., Afshar, S., Tapson, J., and Van Schaik, A. Emnist: Extending mnist to handwritten letters. In *2017 international joint conference on neural networks (IJCNN)*, pp. 2921–2926. IEEE, 2017.
- Fang, M., Cao, X., Jia, J., and Gong, N. Z. Local model poisoning attacks to byzantine-robust federated learning. In *Proceedings of the 29th USENIX Conference on Security Symposium*, pp. 1623–1640, 2020.
- Fung, C., Yoon, C. J., and Beschastnikh, I. The limitations of federated learning in sybil settings. In *RAID*, pp. 301–316, 2020.
- Geiping, J., Bauermeister, H., Dröge, H., and Moeller, M. Inverting gradients-how easy is it to break privacy in federated learning? *Advances in Neural Information Processing Systems*, 33:16937–16947, 2020.
- Gu, T., Liu, K., Dolan-Gavitt, B., and Garg, S. Badnets: Evaluating backdooring attacks on deep neural networks. *IEEE Access*, 7:47230–47244, 2019.
- Guerraoui, R., Rouault, S., et al. The hidden vulnerability of distributed learning in byzantium. In *International Conference on Machine Learning*, pp. 3521–3530. PMLR, 2018.
- He, K., Fan, H., Wu, Y., Xie, S., and Girshick, R. Momentum contrast for unsupervised visual representation learning. In *Proceedings of the IEEE/CVF conference on computer vision and pattern recognition*, pp. 9729–9738, 2020.
- Hsu, T.-M. H., Qi, H., and Brown, M. Measuring the effects of non-identical data distribution for federated visual classification. *arXiv preprint arXiv:1909.06335*, 2019.
- Khosla, P., Teterwak, P., Wang, C., Sarna, A., Tian, Y., Isola, P., Maschinot, A., Liu, C., and Krishnan, D. Supervised contrastive learning. *Advances in Neural Information Processing Systems*, 33:18661–18673, 2020.

- Kirkpatrick, J., Pascanu, R., Rabinowitz, N., Veness, J., Desjardins, G., Rusu, A. A., Milan, K., Quan, J., Ramalho, T., Grabska-Barwinska, A., Hassabis, D., Clopath, C., Kumaran, D., and Hadsell, R. Overcoming catastrophic forgetting in neural networks. *Proceedings of the National Academy of Sciences*, 114(13):3521–3526, 2017. doi: 10.1073/pnas.1611835114.
- Krizhevsky, A., Nair, V., and Hinton, G. Cifar-10 (canadian institute for advanced research).
- Krizhevsky, A., Hinton, G., et al. Learning multiple layers of features from tiny images. 2009.
- Li, T., Sahu, A. K., Zaheer, M., Sanjabi, M., Talwalkar, A., and Smith, V. Federated optimization in heterogeneous networks. *Proceedings of Machine Learning and Systems*, 2:429–450, 2020.
- Liu, Y., Ma, S., Aafer, Y., Lee, W.-C., Zhai, J., Wang, W., and Zhang, X. Trojaning attack on neural networks. 2017.
- Liu, Y., Ma, X., Bailey, J., and Lu, F. Reflection backdoor: A natural backdoor attack on deep neural networks. In *Computer Vision—ECCV 2020: 16th European Conference, Glasgow, UK, August 23–28, 2020, Proceedings, Part X 16*, pp. 182–199. Springer, 2020.
- Lyu, L., Yu, H., Ma, X., Chen, C., Sun, L., Zhao, J., Yang, Q., and Philip, S. Y. Privacy and robustness in federated learning: Attacks and defenses. *IEEE transactions on neural networks and learning systems*, 2022.
- McMahan, B., Moore, E., Ramage, D., Hampson, S., and y Arcas, B. A. Communication-efficient learning of deep networks from decentralized data. In *Artificial intelligence and statistics*, pp. 1273–1282. PMLR, 2017.
- Naseri, M., Hayes, J., and De Cristofaro, E. Local and central differential privacy for robustness and privacy in federated learning. In *NDSS*, 2022.
- Nasr, M., Shokri, R., and Houmansadr, A. Comprehensive privacy analysis of deep learning: Passive and active white-box inference attacks against centralized and federated learning. In *2019 IEEE symposium on security and privacy (SP)*, pp. 739–753. IEEE, 2019.
- Nguyen, T. D., Rieger, P., Chen, H., Yalame, H., Möllering, H., Fereidooni, H., Marchal, S., Miettinen, M., Mirhoseini, A., Zeitouni, S., et al. {FLAME}: Taming backdoors in federated learning. In *31st USENIX Security Symposium (USENIX Security 22)*, pp. 1415–1432, 2022.
- Rieger, P., Krauß, T., Miettinen, M., Dmitrienko, A., and Sadeghi, A.-R. Close the gate: Detecting backdoored models in federated learning based on client-side deep layer output analysis. *arXiv preprint arXiv:2210.07714*, 2022a.
- Rieger, P., Nguyen, T. D., Miettinen, M., and Sadeghi, A.-R. Deepsight: Mitigating backdoor attacks in federated learning through deep model inspection. In *NDSS*, 2022b.
- Saha, A., Subramanya, A., and Pirsiavash, H. Hidden trigger backdoor attacks. In *Proceedings of the AAAI conference on artificial intelligence*, volume 34, pp. 11957–11965, 2020.
- Shafahi, A., Huang, W. R., Najibi, M., Suci, O., Studer, C., Dumitras, T., and Goldstein, T. Poison frogs! targeted clean-label poisoning attacks on neural networks. *Advances in neural information processing systems*, 31, 2018.
- Shejwalkar, V. and Houmansadr, A. Manipulating the byzantine: Optimizing model poisoning attacks and defenses for federated learning. In *NDSS*, 2021.
- Shejwalkar, V., Houmansadr, A., Kairouz, P., and Ramage, D. Back to the drawing board: A critical evaluation of poisoning attacks on production federated learning. In *2022 IEEE Symposium on Security and Privacy (SP)*, pp. 1354–1371. IEEE, 2022.
- Shen, S., Tople, S., and Saxena, P. Auror: Defending against poisoning attacks in collaborative deep learning systems. In *Proceedings of the 32nd Annual Conference on Computer Security Applications*, pp. 508–519, 2016.
- Sun, Z., Kairouz, P., Suresh, A. T., and McMahan, H. B. Can you really backdoor federated learning? *CoRR*, abs/1911.07963, 2019.
- Tang, D., Wang, X., Tang, H., and Zhang, K. Demon in the variant: Statistical analysis of dnns for robust backdoor contamination detection. In *USENIX Security Symposium*, pp. 1541–1558, 2021.
- Van der Maaten, L. and Hinton, G. Visualizing data using t-sne. *Journal of machine learning research*, 9(11), 2008.
- Wang, H., Sreenivasan, K., Rajput, S., Vishwakarma, H., Agarwal, S., Sohn, J.-y., Lee, K., and Papailiopoulos, D. Attack of the tails: Yes, you really can backdoor federated learning. In Larochelle, H., Ranzato, M., Hadsell, R., Balcan, M., and Lin, H. (eds.), *Advances in Neural Information Processing Systems*, volume 33, pp. 16070–16084. Curran Associates, Inc., 2020.
- Wen, Y., Geiping, J., Fowl, L., Souri, H., Chellappa, R., Goldblum, M., and Goldstein, T. Thinking two moves ahead: Anticipating other users improves backdoor attacks in federated learning. *arXiv preprint arXiv:2210.09305*, 2022.
- Xie, C., Huang, K., Chen, P.-Y., and Li, B. Dba: Distributed backdoor attacks against federated learning. In *International Conference on Learning Representations*, 2019.

- Xie, C., Chen, M., Chen, P.-Y., and Li, B. Crfl: Certifiably robust federated learning against backdoor attacks. In *International Conference on Machine Learning*, pp. 11372–11382. PMLR, 2021.
- Yin, D., Chen, Y., Kannan, R., and Bartlett, P. Byzantine-robust distributed learning: Towards optimal statistical rates. In *International Conference on Machine Learning*, pp. 5650–5659. PMLR, 2018.
- Zhang, Z., Panda, A., Song, L., Yang, Y., Mahoney, M., Mittal, P., Kannan, R., and Gonzalez, J. Neurotoxin: Durable backdoors in federated learning. In Chaudhuri, K., Jegelka, S., Song, L., Szepesvari, C., Niu, G., and Sabato, S. (eds.), *Proceedings of the 39th International Conference on Machine Learning*, volume 162 of *Proceedings of Machine Learning Research*, pp. 26429–26446. PMLR, 17–23 Jul 2022.
- Zhao, L., Hu, S., Wang, Q., Jiang, J., Shen, C., Luo, X., and Hu, P. Shielding collaborative learning: Mitigating poisoning attacks through client-side detection. *IEEE Transactions on Dependable and Secure Computing*, 18(5):2029–2041, 2020.

A. Complementary experiment results

In this section, we will provide experimental results and analysis of all the tasks which are not presented in the main text and summarize the lifespan of all the tasks under different attack methods to further prove the superiority of our proposed method.

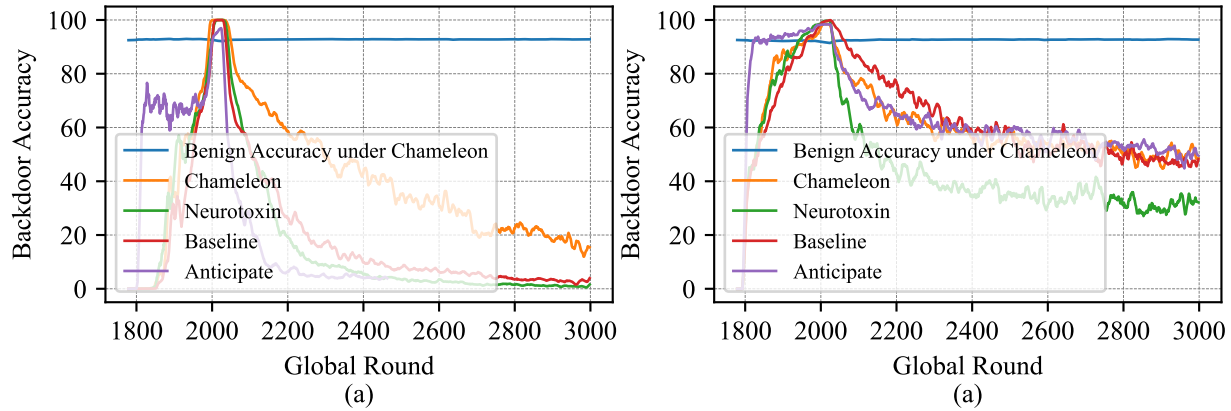


Figure 12. Backdoor accuracy on CIFAR10 with (a) green-car, (b) southwest airline images from edge-case dataset. For all tasks, the attack starts at round 1800, and lasts for AttackNum=230 rounds.

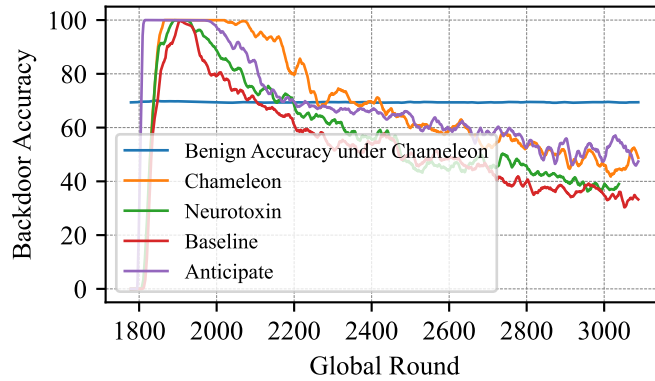


Figure 13. Backdoor accuracy on CIFAR100 with truck-with-vertically-striped-walls-in-the-background. For all tasks, the attack starts at round 1800, and lasts for AttackNum=100 rounds.

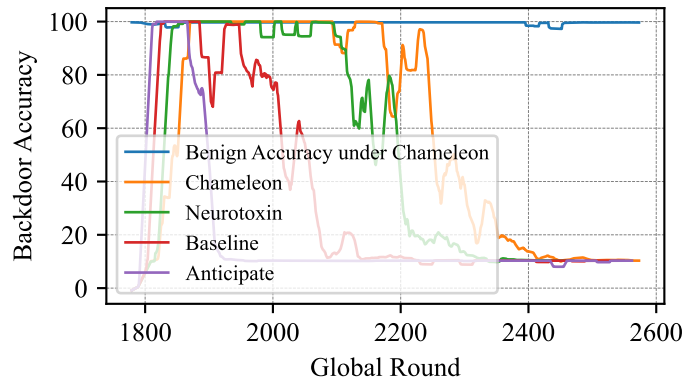


Figure 14. Backdoor accuracy on EMNIST with type-1 pixel-pattern backdoor. For all tasks, the attack starts at round 1800, and lasts for AttackNum=60 rounds.

Table 6. Lifespan $L(\gamma)$ of the backdoor inserted by Chameleon, Anticipate, Neurotoxin and baseline of all tasks evaluated in this paper. The model architecture used here is ResNet18.

Datasets	Backdoor	AttckNum	Chameleon	Anticipate	Neurotoxin	Baseline
EMNIST	Type-1 pixel-pattern	60	427(50%)	40(50%)	336(50%)	193(50%)
CIFAR10	Type-1 pixel-pattern	40	1501(50%)	837(50%)	1068(50%)	912(50%)
CIFAR10	Type-2 pixel-pattern $p_d = 0.1$	40	833(50%)	358(50%)	664(50%)	646(50%)
CIFAR10	Type-2 pixel-pattern $p_d = 0.5$	40	720(50%)	498(50%)	545(50%)	438(50%)
CIFAR10	car with striped bg	230	1106(50%)	283(50%)	216(50%)	205(50%)
CIFAR10	green car	230	264(50%)	20(50%)	76(50%)	74(50%)
CIFAR10	racing car	230	208(50%)	5(50%)	40(50%)	70(50%)
CIFAR10	southwest airline (edge-case)	230	339(60%)	349(60%)	75(60%)	336(60%)
CIFAR100	truck with striped bg	100	625(60%)	623(60%)	297(60%)	170(60%)
CIFAR100	bicycle with black bg	150	661(50%)	229(50%)	112(50%)	133(50%)

Table 7. Lifespan $L(\gamma)$ of the backdoor inserted by Chameleon, Anticipate, Neurotoxin and baseline with ResNet34 model architecture in this paper.

Datasets	Backdoor	AttackNum	Chameleon	Anticipate	Neurotoxin	Baseline
CIFAR10	racing car	230	567(40%)	355(40%)	7(40%)	13(40%)

We present the rest of the experiment results in Figure 12, Figure 13, Figure 14, and summarize the lifespans of all the evaluated tasks in Table 6 and Table 7.

As it is shown in Table 6, lifespans of the backdoors inserted using Chameleon achieve the highest compared to other methods except for the edge-case backdoor where Chameleon achieves a comparable 60%-Lifespan with Anticipate. Comparing the lifespans of semantic backdoors in CIFAR10 and CIFAR100, we can see that the attacker can plant more durable semantic backdoors into CIFAR100 tasks than CIFAR10 tasks with even less AttackNum required. Also, the edge-case backdoor has stronger durability than other semantic backdoors in CIFAR10 on average. For CIFAR100 tasks, this is because CIFAR100 has more categories in the dataset, which lowers the probability of interferers being selected into the dataset of following benign clients. Following uploaded benign updates will have less conflict with the inserted backdoor, and thus improve durability. Similarly, edge-case backdoor images in CIFAR10 which live on the tail of the input distribution have less in common with interferer images. Thus, future benign updates trained by interferers will also have less conflict with the embedded backdoor, which extends the lifespan of the backdoor compared to other CIFAR10 semantic backdoors.

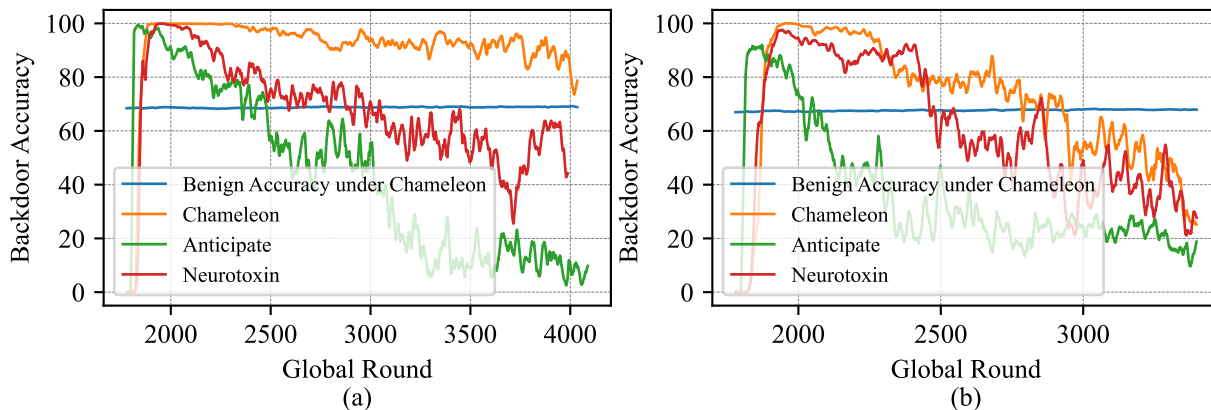


Figure 15. Backdoor accuracy when attacking (a) VGG16, (b) VGG19. For all tasks, the attack starts at round 1800, and lasts for AttackNum=150 rounds. The evaluated backdoor is bicycle-with-black-background.

We further provide more experimental results to verify that Chameleon is less sensitive to the changes of model architectures. Figure 15 and Table 8 show that the durability of the backdoor inserted by Chameleon achieves the strongest durability when

Chameleon: Adapting to Peer Images for Planting Durable Backdoors in Federated Learning

Table 8. 50%-Lifespan of the backdoor inserted by Chameleon, Anticipate and Neurotoxin with VGG16 and VGG19.

Model	Chameleon	Anticipate	Neurotoxin
VGG16	2050	237	530
VGG19	731	26	489

attacking VGG16 or VGG19, which further shows that our method performs well under a wide range of model architectures.